Journal of Solid State Chemistry **163,** 377–384 (2002)
doi:10.1006/jssc.2001.9367, available online at http://www.idealibrary.com on IDEAL®

Structural Characterization of $YMe_xMn_{1-x}O_3$ (*Me* = Cu, Ni, Co) Perovskites

Carlos Moure,*[,1] Dionisio Gutierrez,* Octavio Peña,† and Pedro Duran*

*Electroceramics Department, Instituto de Ceramica y Vidrio, CSIC, 28500 Arganda, Madrid, Spain; and †LCSIM/UMR6511-CNRS, Université de Rennes I, Rennes, France

Received June 14, 2001; in revised form August 13, 2001; accepted August 17, 2001; published online November 27, 2001

The structural properties of the $YMe_xMn_{1-x}O_3$ (*Me* = Cu, Ni, Co) pseudobinary oxides have been studied by X-ray diffraction and electrical measurements. The powders were prepared by solid state reaction between the corresponding oxides. The incorporation in solid solution of small divalent cations, Cu^{2+}, Ni^{2+}, and Co^{2+}, substituting for Mn in the hexagonal $YMnO_3$ compound, leads to a phase transition in which a perovskite-type structure is formed. The amount of substituting cation necessary for such a transition depends on the cation nature and, to a small extent, on the ionic radius. The phase transition depends strongly on the progressive substitution of the Jahn–Teller Mn^{3+} cation and therefore of the cooperative Jahn–Teller interaction weakness. The steric influence plays a secondary role, as is shown by the very small variation of the tolerance factor, *t*, as a function of the cation content. The solid solutions with perovskite-type structure show semiconducting behavior. The conductivity mechanism is of a thermally activated small polaron hopping.

Key Words: **manganites; perovskite solid solutions; crystalline structure; electrical properties.**

1. INTRODUCTION

The mixed oxides of general formula $LnMeO_3$, where *Ln* is a rare earth, (RE) ion and *Me* = Fe, Cr, Ti, V, Rh, belong to the group of orthorhombic distorted perovskites, which crystallize in the space group (S.G.) *Pbnm*. When *Me* = Mn, the $LnMnO_3$ compounds show the orthorhombic distorted perovskite structure only up to the Dy cation, whereas the compounds corresponding to RE with smaller ionic radii, from Er to Y, crystallize with a hexagonal-type structure and S.G. $P6_3cm$ (1).

[1]To whom correspondence should be addressed at Electroceramics Department, Instituto de Ceramica y Vidrio, CSIC, 28500 Arganda del Rey, Madrid, Spain. Fax: 34 91 870 0550. E-mail: cmoure@icv.csic.es.

As is well known, the distortion degree of the perovskite structure in ABO_3 compounds depends, between other causes, on steric effects, associated with changes in the ionic radius of the component *A* and *B* cations. This contribution is well represented by the Goldschmidt tolerance factor $\mathbf{t} = (r_A + r_O)/(r_B + r_O)^*\sqrt{2}$, where r_A represents the ionic radius of the large *A* cation (*Ln* in the present case), r_B represents the ionic radius of the small *B* cation, (Fe, Cr, Mn, Ti, and others for the above-mentioned compounds), and r_O is the ionic radius of O^{2-}. When the tolerance factor decreases, the distortion degree increases (2). Nevertheless, in the case of the manganite compounds, $LnMnO_3$, another factor must be considered with regard to the structure distortion. Thus, the Jahn–Teller nature of the Mn^{3+} cation induces an additional axial distortion effect, which is cooperative (3). Consequently, a combination of low **t** values and Jahn–Teller effect leads to a modification of the structure, from perovskite-type to the hexagonal-type structure mentioned above, with a higher grade of distortion with respect to the orthorhombic perovskites. This is the reason that compounds such as $YFeO_3$ and $YMnO_3$ that have the same **t** value (0.835), owing to the equality between the ionic radius of Fe^{3+} and Mn^{3+} cations, show very different structures.

As also indicated above, $YMnO_3$ crystallizes in the hexagonal S.G. $P6_3cm$ (4). The Y^{3+} cation is sevenfold coordinated with oxygen ions while the Mn^{3+} cation is pentacoordinated with O^{2-}. It is possible to obtain solid solution in the compositional range $\sim$ 25 to 100 mol% with the $CaMnO_3$ compound, which crystallizes with a perovskite-type structure and S.G. *Pbnm* (5). According to Vega *et al.* (6), two phase transitions can be observed at room temperature in this solid solution when the Ca content increases. The first one is a transition from a hexagonal-type structure to an orthorhombic perovskite-type structure (O′-type structure, with $c/\sqrt{2} < a < b$) occurring for Ca content $\sim$ 25 at.%. The second one is a phase transition from O′ to O phase (orthorhombic O-type structure, with $a < c/\sqrt{2} < b$), which takes place for Ca content of $\sim$ 50

0022-4596/02 $35.00

at.%. The transition to a perovskite-type phase can be attributed, in a first approximation, to an increase of the tolerance factor caused by the incorporation of a larger cation such as Ca^{2+} in the *A* lattice site substituting for a smaller Y^{3+} cation. On the other hand, it has been observed that the solid solution in the $YNi_xMn_{1-x}O_3$ pseudobinary oxides also shows a phase transition from hexagonal $YMnO_3$ type to orthorhombic perovskite type. The phase transition takes place at $x \leq 0.20$ (7). This phase transition occurs with a small change of the tolerance factor and for a content of the modifying cation lower than that of the (Y,Ca)MnO_3 system. Therefore, it was pointed out that the transition from hexagonal to orthorhombic structure is caused preferentially by the partial disappearance of Mn^{3+} from the crystalline lattice, which takes place by two mechanisms: (a) direct substitution of Ni^{2+} for Mn^{3+} and (b) change of Mn^{3+} to Mn^{4+} in an equivalent amount to the incorporated Ni^{2+}, to preserve the valence equilibrium.

In the present work the crystalline characteristics of solid solutions in three pseudobinary oxides, based on the $YMnO_3$, modified by Ni^{2+}, Cu^{2+}, and Co^{2+}, are examined as a function of the nature of each cation. Relationships between **t**, Mn^{3+} content, and phase transitions are discussed. Electrical transport properties are also presented.

2. EXPERIMENTAL

$Y(Ni_xMn_{1-x})O_3$, $Y(Cu_xMn_{1-x})O_3$, and $Y(Co_xMn_{1-x})O_3$ compositions with $x = 0.10$–0.70 were prepared by solid state reaction between stoichiometric mixtures, using MnO, CoO, NiO, CuO, and Y_2O_3 reagent-grade oxides with submicronic particle size as raw materials. The mixtures were homogenized by wet attrition milling, using isopropanol as the liquid medium. The dried mixtures were calcined at 1000°C for 2 h. The calcined samples were milled again by the same technique, dried, granulated, and uniaxially pressed. Granulometric analysis was carried out on the synthesized powders by means of laser counting (Mastersizer model, Malvern Instruments, Ltd, U.K.) and BET techniques (Quantachrome MS-16 model, Syosset, NY). Pressed pellets were sintered between 1150 and 1425°C for 2 h. All the samples were treated with the same thermal cycle of heating, 3°C/min, and cooling, 1°C/min, to compare the respective results, with regard to the redox equilibrium. The Cu-containing solid solutions were sintered at the lower temperature, whereas the Ni-containing solid solutions were sintered at the higher temperature. XRD analysis was performed both on the calcined powders and on the sintered samples using a D-5000 Siemens Diffractometer and Cu$K\alpha$ radiation. The powder was identified by scanning at a rate of 2° 2θ/min, and the lattice parameters were calculated from the spectra obtained on the sintered and reground samples at a scanning rate of $\frac{1}{4}^\circ$ 2θ/min. Powder of Si was employed as an internal standard. The Goldschmidt tolerance factor **t** has been calculated using the ionic radii tabulated by Shannon (8), taking into account the oxygen coordination of the involved cations and the existence of different valence states of the Mn and the modifying cations, with different ionic radii, in the solid solutions. A mean ionic radius on *B* lattice sites has been used when two or more cations are present on those sites.

Bar-shaped samples were painted with silver paste, which was fired at 800°C for 1 h. Four-points dc conductivity measurements were carried out for all the solid solutions having perovskite-type structure, between 25 and 700°C. For measurements, a Constant Current dc power supply (Tektronix, model PS280) and a HP Multimeter (model 44201A), with 1 μA dc current resolution were used. Activation energies were calculated from the corresponding Arrhenius plots. The Seebeck coefficient measurements were made on cylindrical samples, 0.3 cm in diameter and 1.5 cm in length, using a quasi-conventional technique for a rapid and qualitative determination of the majority charge-carrier sign (9). For the measurements, two metal blocks containing the thermocouples held the sample. A heater on one block produced the temperature gradient in the sample. The thermoelectric voltage was measured between the same reference points.

3. RESULTS AND DISCUSSION

The apparent particle size, as measured by laser counting, was ~ 2.0 μm, but this size corresponds to that of aggregates in all the systems. The BET measurements indicated specific surface area values of $\sim 4.0\ m^2/g$, which correlates well with an average particle size of ~ 0.21 μm for all the synthesized powders.

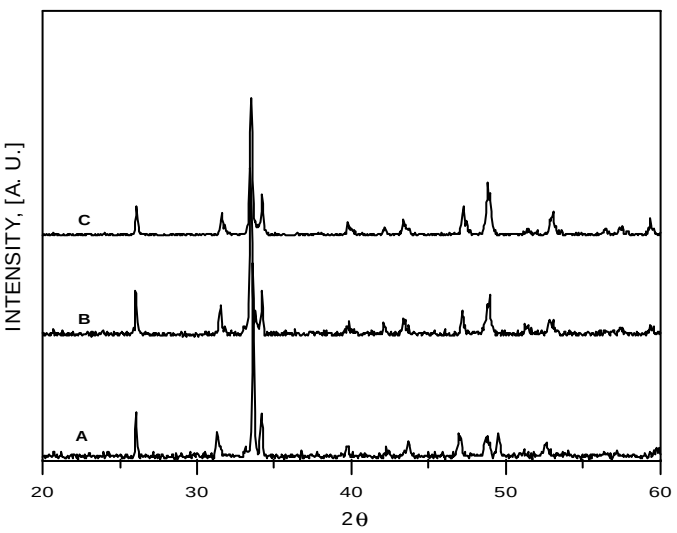

FIG. 1. XRD patterns of compositions with the minimum content of substituting cation needed to obtain monophasic samples: (A) 30 at.% of Cu; (B) 20 at.% of Ni; (C) 25 at.% of Co.

Figure 1 shows the XRD diffraction patterns of samples corresponding to compositions of the different pseudo-binary oxides with the minimum content needed to obtain pure perovskite phase, such as is indicated in the following paragraph. All the patterns were indexed as orthorhombic perovskites with S.G. Pbnm

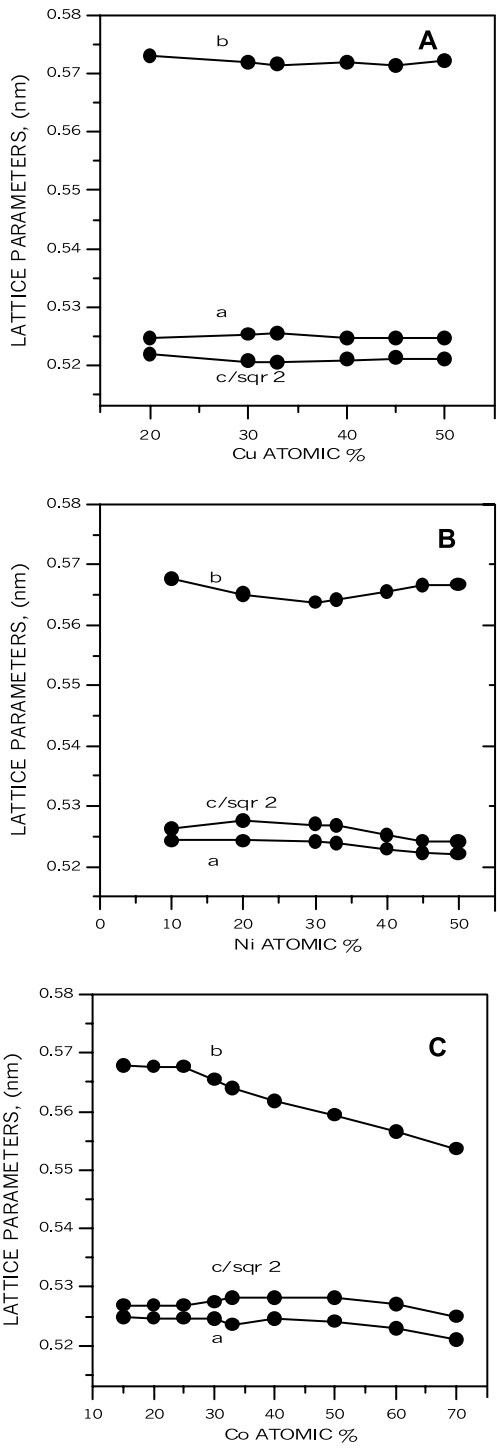

FIG. 2. Concentration dependence of the lattice parameters of (A) $Y(Cu,Mn)O_3$ solid solution, (B) $Y(Ni,Mn)O_3$ solid solution, and (C) $Y(Co,Mn)O_3$ solid solution.

TABLE 1
Lattice Parameters of the Solid Solution $Y(Cu_xMn_{1-x})O_3$

at.% Cu	0[a]	20[b]	30	33	40	45	50
a (nm) ($\pm$ 0.0001)	0.6136	0.5246	0.5253	0.5255	0.5247	0.5247	0.5246
b (nm) ($\pm$ 0.0001)		0.5730	0.5719	0.5715	0.5718	0.5714	0.5722
c (nm) ($\pm$ 0.0001)	1.1400	0.7382	0.7363	0.7362	0.7367	0.7371	0.7368
b/a		1.092	1.089	1.088	1.090	1.089	1.091
V (nm^3) ($\pm$ 0.0004)	0.3720	0.2219	0.2212	0.2211	0.2211	0.2210	0.2212

[a]Hexagonal lattice, $Z = 6$.
[b]Biphasic region.

Figures 2A–2C show the variation of the lattice parameters calculated from the XRD patterns of the solid solutions corresponding to the different modifying cations. Only lattice parameters of the perovskite-type phases are displayed, even for the two-phase region. $c/\sqrt{2}$ is represented in place of the c parameter. It can be seen that the cation amount, which induces phase transition from hexagonal type to perovskite type, varies for each cation. Thus, ≤ 20 at.% of Ni^{2+}, ≤ 25 at.% of Co^{2+}, and ≤ 30 at.% of Cu^{2+} are the approximate contents from what the phase transition takes place. Below these contents, two-phase regions are observed in which a majority $YMnO_3$ phase coexists with minority amounts of a perovskite-type phase. Above 50 at.% of Ni^{2+} and of Cu^{2+}, the perovskite phase coexists with Y_2O_3 and with $Y_2O_3 + Y_2Cu_2O_5$, respectively. On the other hand, the range of solid solution for the Co-containing system is extended at least up to 70 at.% of Co. The perovskite structures are orthorhombic O-type, with $a < c/\sqrt{2} < b$ in the systems containing Ni and Co, whereas it is of the O′-type, with $c/\sqrt{2} < a < b$ in the case of the Cu-containing solid solutions, such as is seen in the figures. Tables 1–3 show these measured lattice parameter values, along with the corresponding orthorhombicity factor, b/a, and the unit cell volume. Lattice parameters and unit cell volume of the $YMnO_3$ phase are also shown.

Such as is seen in Fig. 3, in all the systems the increase of the modifying cation leads to a decrease of the perovskite unit cell. This decrease is more pronounced when the ionic radius of the cation decreases.

Figure 4 depicts the tolerance factor, **t**, vs the cation content for all the systems. For comparison, the curve corresponding to the $(Y,Ca)MnO_3$ solid solution is also represented. Figure 5 shows the a, b, and c lattice parameters as a function of the ionic radius of the different cations for the intermediate 33/67 Me/Mn ratio compositions.

As can be seen, the lower amount necessary to induce a phase transition from a hexagonal-type to a perovskite-type structure corresponds to the Ni^{2+} cation, in spite of

TABLE 2
Lattice Parameters of the Solid Solutions $Y(Ni_xMn_{1-x})O_3$

At. % Ni	0[a]	10[b]	20	30	33	40	45	50
a (nm) ($\pm$ 0.0001)	0.6136	0.5243	0.5243	0.5241	0.5239	0.5229	0.5223	0.5221
b (nm) ($\pm$ 0.0001)		0.5677	0.5651	0.5638	0.5641	0.5656	0.5666	0.5667
c (nm) ($\pm$ 0.0001)	1.1400	0.7443	0.7460	0.7452	0.7449	0.7427	0.7414	0.7412
b/a		1.083	1.078	1.076	1.077	1.082	1.085	1.086
V (nm^3) ($\pm$ 0.0004)	0.3720	0.2215	0.2211	0.2202	0.2202	0.2196	0.2194	0.2193

[a]Hexagonal lattice, $Z = 6$.
[b]Biphasic region

the higher tolerance factor that shows the solid solution $Y(Co,Mn)O_3$ for all the compositions with the same content of the modifying cation. On the other hand, Cu-containing solid solutions are those that need the higher amount of modifying cation to attain a single-phase perovskite structure. The reasons for these behaviors can be based on the following features of each cation: The Cu^{2+} cation is a Jahn–Teller-type cation, such as the Mn^{3+}. If it is supposed that the Jahn–Teller effect is the main cause of the hexagonal distortion, the number of Jahn–Teller cations that disappear for each Cu cation substituting to a Mn cation is lower than that of the other systems. Therefore, a higher amount of Cu will be necessary to induce the phase transition. On the other hand, even in the perovskite-type structure, a relatively higher number of Jahn–Teller cations remains on the lattice, with respect to that of the Ni- and Co-containing systems. Therefore, it can be considered that a relatively high cooperation distortion effect still acts on the crystalline lattice. This could be the explanation for the appearance of the O′-type orthorhombic perovskite in the solid solution $Y(Cu,Mn)O_3$ because this O′ phase is the most distorted perovskite-type one. The high value of the orthorhombicity coefficient b/a measured on these solid solutions and the small decrease of the cell volume corroborates this hypothesis.

The system $Y(Co,Mn)O_3$ shows a wider range of solid solution. This is extended at least up to 70 at.% of Co content, such as what has been observed in the present study. The compositions above 50 at.% of Co are more sensitive to the synthesis and sintering processes than those with Co content below 50 at.% Co. The Co cation shows two stable valence states, $+2$ and $+3$. Therefore, the following cation configuration can be postulated

$$Y[Co^{2+}_{1-x}Mn^{4+}_{1-x}Co^{3+}_{2x-1}]O_3 \qquad [1]$$

when $x \geq 0.5$. Actually, the presence of Co^{3+} cation in the solid solution could be extended to the compositions with $x \leq 0.5$, and it would be a function of the thermal story of the solid solutions. This hypothesis can be the reason for the higher value of the Co content to attain a perovskite-type solid solution when compared to the Ni-containing system in spite of the higher tolerance factor that this Co-containing system shows. Thus, the presence of Co^{3+} induces a lower amount of Mn^{4+} in the lattice and, therefore, a higher content of Mn^{3+} remains in the compound. Consequently, a higher amount of substituting cation will be necessary to attain the same result than that corresponding to the Ni system. The cell volume decreases at faster rate than that of the $Y(Cu,Mn)O_3$ system, and the decrease is

TABLE 3
Lattice Parameters of the Solid Solution $Y(Co_xMn_{1-x})O_3$

at.% Co	0[a]	15[b]	20[b]	25	30	33	40	50	60	70
a (nm) ($\pm$ 0.0001)	0.6136	0.5248	0.5247	0.5247	0.5245	0.5236	0.5245	0.5241	0.5229	0.5210
b ($\pm$ 0.0001)		0.5678	0.5677	0.5677	0.5654	0.5640	0.5618	0.5594	0.5565	0.5536
c ($\pm$ 0.0001)	1.1400	0.7452	0.7452	0.7452	0.7460	0.7468	0.7470	0.7468	0.7454	0.7424
b/a		1.0819	1.0819	1.0819	1.0779	1.0771	1.0711	1.0673	1.0642	1.0626
V (nm^3) ($\pm$ 0.0004)	0.3720	0.2221	0.2220	0.2219	0.2212	0.2206	0.2201	0.2189	0.2169	0.2141

[a]Hexagonal lattice, $Z = 6$.
[b]Biphasic region.

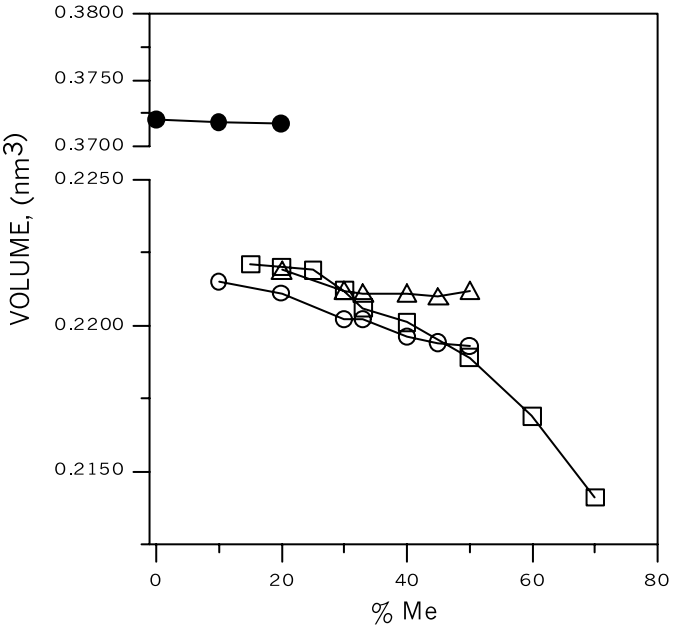

FIG. 3. Variation of one-formula unit volume as a function of x for the different substituting cations, *Me*: (△) $Me = Cu$; (○) $Me = Ni$; (□) $Me = Co$; (●) $YMnO_3$ phase (for $Me = Cu,Co$).

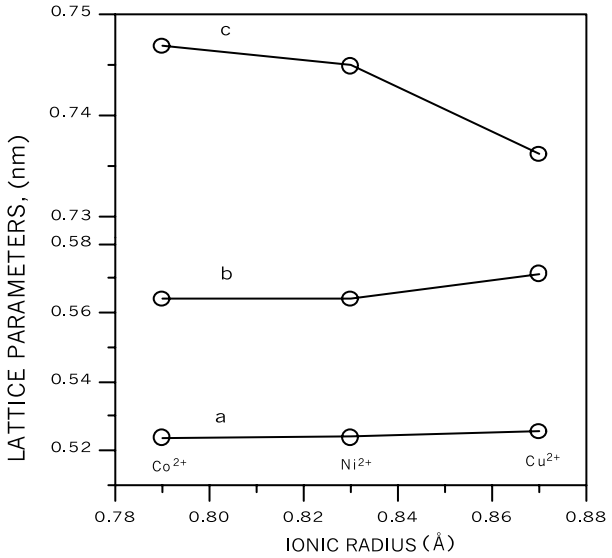

FIG. 5. Variation of lattice parameters vs ionic radius of modifying cation for the $YMe_{0.33}Mn_{0.67}O_3$, Me = Cu, Ni, Co compositions.

more pronounced when $x > 0.50$ and, according to [1], no Mn^{3+} is present.

The $Y(Ni,Mn)O_3$ system shows an upper limit to the solid solutions located like the $Y(Cu,Mn)O_3$ system at 50 at.% of Ni. Above this amount, the presence of Y_2O_3 phase is observed in spite of the thermal treatment. On the other hand, this system showed the lower limit of modifying cation needed to produce the phase transition hexagonal type → perovskite type. The reason for this behavior can be attributed to the high stability of the Ni^{2+} valence state, which inhibits the possible formation of a cation configuration such as that represented in the formula [1] for the Co-containing system, and induces the formation of the same amount of Mn^{4+} cation for each Ni^{2+} cation incorporated in the lattice.

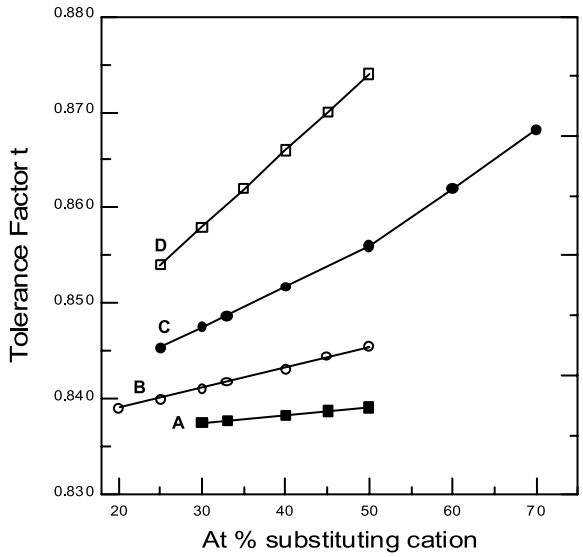

FIG. 4. Concentration dependence of the tolerance factor, **t**: (A) $Y(Cu,Mn)O_3$ solid solution; (B) $Y(Ni,Mn)O_3$ solid solution; (C) $Y(Co,Mn)O_3$ solid solution; (D) $(Y,Ca)MnO_3$ solid solution.

As seen in Fig. 4, the calculated **t** tolerance factor for all the solid solutions, which increases when the ionic radius of the substituting cation decreases, shows good correlation with the orthorhombicity factor of those ones (Tables 1–3). Higher **t** values correspond to solid solutions with a lower b/a ratio. It is interesting to indicate that the **t** value of the Cu-containing solid solutions with perovskite-type structure (which ranges from 0.837 to 0.839) is practically the same corresponding to a hypothetical $YMnO_3$ double oxide with perovskite-type structure ($\mathbf{t} = 0.835$). The $Y(Cu,Mn)O_3$ solid solution that shows such a low tolerance factor presents also the most distorted perovskite structure, i.e., the O′-type orthorhombic structure, of the three studied.

There is no significative difference between the tolerance factors of the Cu- and Ni-containing solid solutions; however, the slope of the curve is higher for Ni compounds. On the other hand, the $Y(Ni,Mn)O_3$ solid solution crystallizes with O-type orthorhombic perovskite-type structure in the whole range of existence of the monophasic field. The $Y(Co,Mn)O_3$ solid solution shows similar behavior. Its **t** factor is the highest of the three solid solution systems and rises more rapidly with the modifying cation. Only the O-type orthorhombic perovskite-type structure is observed,

in a manner similar to the Ni-containing system, in the whole range of solid solution, extended upto 70 at.% of Co. Finally, it must be mentioned that the $GdMnO_3$ compound has a O′-type structure, in spite of a **t** value of 0.85, which is higher than those corresponding to all the studied solid solutions with $x = 0.30$ for which the perovskite-type phase has been formed in all the systems. That compound has, obviously, 100 at.% of Mn^{3+}, whereas the O-type perovskite structure compounds of the studied systems, such as the $YNi_{0.2}Mn_{0.8}O_3$ solid solution, has $\mathbf{t} = 0.84$, but a lower amount of Mn^{3+}, 60 at.%. This indicates that the most important factor for inducing the phase transition of the hexagonal- to perovskite-type structure is the disappearance of the cooperative Jahn–Teller effect because of the progressive transformation of $Mn^{3+} \rightarrow Mn^{4+}$ induced by the incorporation of a divalent cation on the *B* sites. The steric factor plays a more secondary role since there exists ternary compounds with perovskite-type structure and very low **t** value in which the presence of Jahn–Teller-type cations, $Mn^{3+} + Cu^{2+}$, is ≤ 70 at.%.

Figure 5 shows the variation of the lattice parameters of the $Y(Me_{0.33}Mn_{0.67})O_3$ solid solution ($Me = Cu^{2+}$, Ni^{2+}, and Co^{2+}) as a function of the ionic radius of each cation. According to the variation of the lattice parameters, it could suppose that the Co^{2+} cation is in the low-spin (LS) state for which the ionic radius is lower than that of Ni^{2+} and Cu^{2+}. It can observed that the *a* and *b* lattice parameters decrease slightly and more pronounced, respectively, with the ionic radius, while the *c* parameter increases when the ionic radius decreases. Thus, it can be stated that the effect on the *B* site of cations with decreasing ionic radius is similar to that produced on the *A* site by cations with increasing ionic radius.

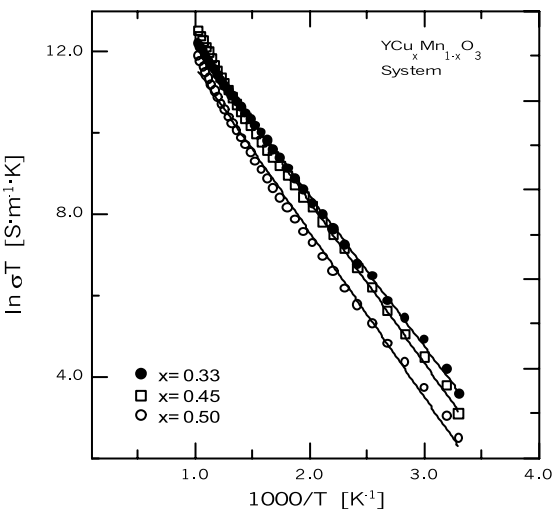

FIG. 6. Log σT vs $1/T$ for different compositions of the $Y(Cu,Mn)O_3$ solid solution.

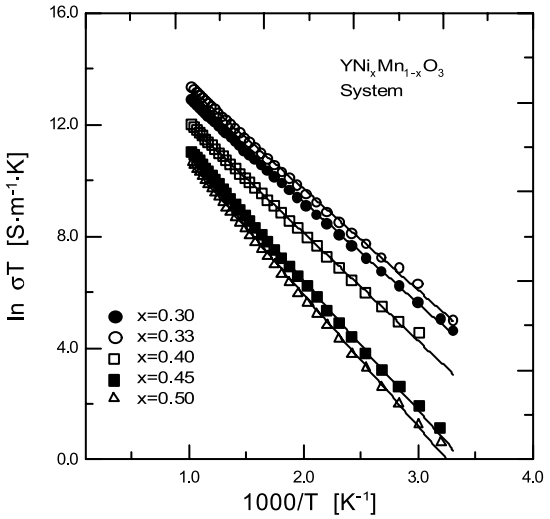

FIG. 7. Log σT vs $1/T$ for different compositions of the $Y(Ni,Mn)O_3$ solid solution.

Electrical measurements have shown semiconducting behavior for all the solid solutions with perovskite-type structure. The conductivity mechanism is of a thermally activated small polaron hopping. Figures 6–8 show Arrhenius plots log σT vs $1/T$. Figures 9–11 depict the results corresponding to the Seebeck coefficient measurements.

From the log σT vs $1/T$ curves one can see that the systems with solid solution limits, i.e., with a high-stability valence state, Cu^{2+} and Ni^{2+}, show an increase of conductivity up to $x = 0.33$ and after a decrease up to $x = 0.50$.

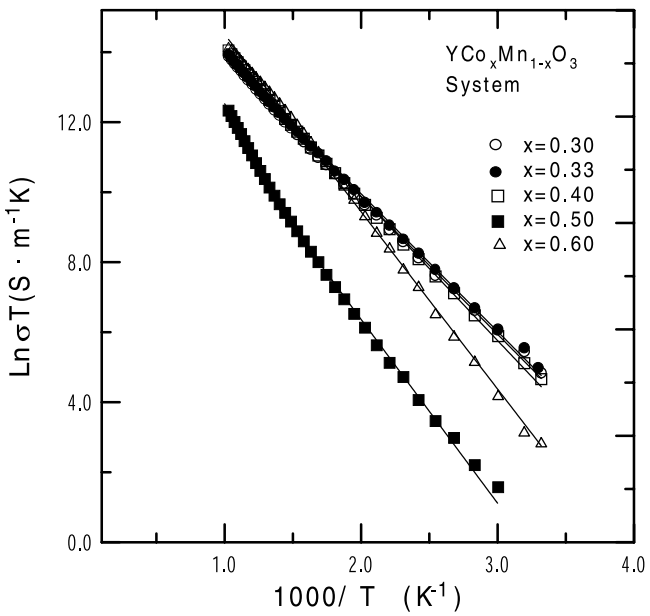

FIG. 8. Log σT vs $1/T$ for different compositions of the $Y(Co,Mn)O_3$ solid solution.

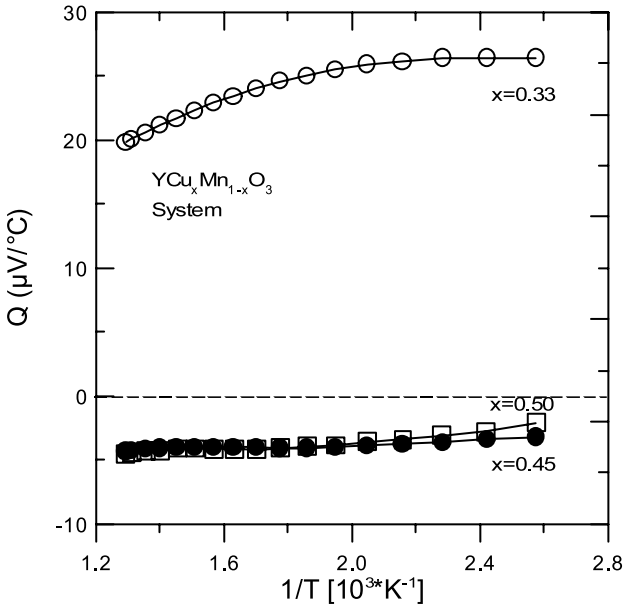

FIG. 9. Seebeck coefficient vs temperature for different compositions of the $Y(Cu,Mn)O_3$ solid solution.

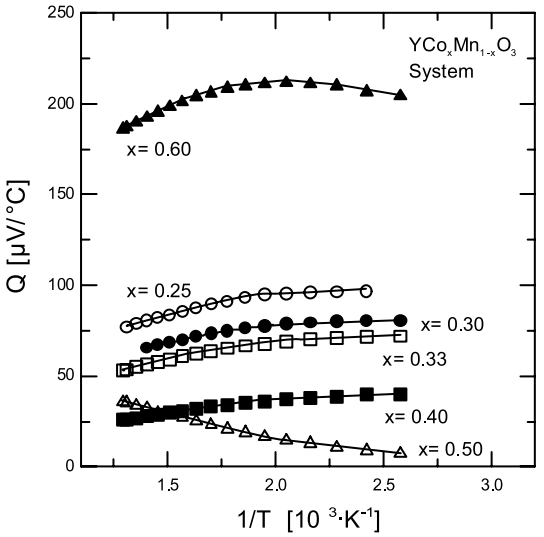

FIG. 11. Seebeck coefficient vs temperature for different compositions of the $Y(Co,Mn)O_3$ solid solution.

Moreover, one can also see, from the Seebeck curves, more or less a remarkable change in the sign of charge carriers for cation contents above 33 at.%. The reason for this behavior could be attributed to the nature of the substituting cations. The Ni^{2+} and Cu^{2+} seem not to contribute to the controlled valence conduction mechanism because of the lack of another valence state of both cations in the nearest neighbor sites. Therefore, the only pairs contributing to the conduction mechanism would be the Mn^{3+}–Mn^{4+} ones. It is easy to see that these possible pairs are increasing up to an amount of 33 at.% *Me* and 67 at.% Mn. A subsequent rise in the *Me* percentage leads to a decrease of the possible forming pairs; it is possible to form 0.30 pairs per formula unit in the 30/70 composition. The number of pairs grows up to 0.33 for 33/67 composition, whereas it is possible to form only 0.2 in the 40/60 composition and 0.1 in the 45/55 one. This variation in the relative percentage between the two Mn cations explains the existence of a maximum in the conductivity values for intermediate Ni, Cu percentages. Besides that, the majority manganese cation for $x \leq 0.33$ is Mn^{3+} and therefore the charge carriers are holes. For $x \geq 0.33$ the majority manganese cation is Mn^{4+} and, consequently, the charge carriers are electrons.

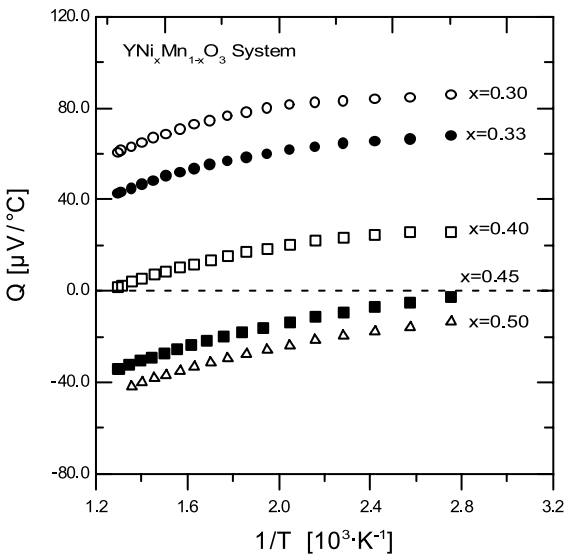

FIG. 10. Seebeck coefficient vs temperature for different compositions of the $Y(Ni,Mn)O_3$ solid solution.

The behavior of the Co-containing solid solutions is something different. Such as that exposed above, it is possible that a part of Co is in the valence state Co^{3+}, thus contributing with the Co^{2+} nearest neighbor to the charge transport mechanism by holes. Therefore, no change in the carrier sign would be appreciated. Nevertheless, the system shows also a maximum in the conductivity value for the same modifying cation content, $x = 0.33$.

4. CONCLUSIONS

The incorporation in solid solution of small divalent cations, Cu^{2+}, Ni^{2+}, and Co^{2+}, substituting for Mn in the hexagonal $YMnO_3$ compound, leads to a phase transition in which a perovskite-type structure is formed. The amount of substituting cation necessary for such a transition

depends on the cation nature and less on the ionic radius. Cations with very stable (II) valence state, (Cu, Ni), show an upper limit to solid solution formation, which has been established at 50 at.%. When the cation is Jahn–Teller type, Cu^{2+}, the lower limit to the appearance of perovskite-type solid solution is higher than that for the other cations.

The phase transition depends strongly on the progressive substitution of the Jahn–Teller Mn^{3+} cation, and therefore of the cooperative interaction weakness. The steric influence plays a secondary role, as is shown by the very slow variation of the tolerance factor, **t**, as a function of the cation content.

The solid solutions with perovskite-type structure show semiconducting behaviors. The conductivity mechanism is of a thermally activated small polaron hopping. For a cation ratio of $\sim 33/67$ Me/Mn, $Me = $ Cu, Ni, a change of sign of the charge carriers has been observed. This was not detected in the Co-containing solid solutions.

ACKNOWLEDGMENT

This work was supported by Spain CICYT-MAT-2000-0815.

REFERENCES

1. O. Muller and R. Roy, *in* "The Major Ternary Structural Families," pp. 357–358. Springer-Verlag, New York, 1974.
2. V. M. Goldschmidt, *Naturwissenschaften* **14,** 477 (1926).
3. J. B. Goodenough, *Phys. Rev.* **100,** 564 (1965).
4. H. L. Yakel, W. C. Koehler, E. F. Bertaut, and E. F. Forrat, *Acta Crystallogr.* **16,** 957, (1963).
5. E. Pollert, S. Kupricka, and E. Kuzmisova, *J. Phys. Chem. Solids* **43,** 1137 (1982).
6. D. Vega, G. Polla, A. G. Leyva, P. Koning, H. Lanza, A. Esteban, H. Aliaga, M. T. Causa, M. Tovar, and B. Alascio, *J. Solid State Chem.* **156,** 458 (2001).
7. D. Gutierrez, O. Peña, J. F. Fernandez, P. Duran, and C. Moure, *J. Eur. Ceram. Soc.*, in press.
8. R. D. Shannon, *Acta Crystallogr. A* **32,** 751 (1976).
9. R. Heikes and R. Ure, *in* "Thermoelectricity: Science and Engineering," pp. 311–322. Interscience, New York, 1961.